Soap-Free Emulsion Copolymerization of Perfluoroalkyl Acrylates in the Presence of a Reactive Surfactant

Yang Tingting,[1] Peng Hui,[1] Cheng Shiyuan,[1] In Jun Park[2]

[1]*School of Chemistry and Materials Science, Hubei University, Wuhan 430062, China*
[2]*Department of Chemistry Engineering, Korea Research Institute of Chemistry Technology, Taejon 305-606, South Korea*

Received 19 October 2005; accepted 14 January 2006
DOI 10.1002/app.24668
Published online in Wiley InterScience (www.interscience.wiley.com).

ABSTRACT: Soap-free emulsion copolymerization of perfluoroalkyl acrylate (FA)/methyl methacrylate (MMA)/*n*-butyl acrylate (*n*-BA) was carried out in the presence of sodium 2-acrylamide-2-methyl propanesulfonate (AMPSNa) as a reactive surfactant and potassium persulfate (KPS) as an initiator. An analysis of the effects of concentration of AMPSNa, KPS, FA as well as polymerization temperature on the kinetic features (rate of polymerization) and colloidal characteristics (mean particle diameter, particle disperse index, particle numbers, and surface charge density) was followed. NMR, FTIR, AFM, and fluorine-selective electrode analysis were used to characterize the composition and morphology of the FA copolymers. Both AFM analysis and contact angle measurements strongly implied that the fluorinated segments migrated to the outmost surface and created films with lower surface energy. © 2007 Wiley Periodicals, Inc. J Appl Polym Sci 104: 2438–2444, 2007

Key words: perfluoroalkyl acrylate; reactive surfactant; soap-free; emulsion copolymerization

INTRODUCTION

It is well-known that fluorinated polymers present a number of interesting and peculiar properties provided mainly by the unique features of fluorine atom and the resulting C—F bond.[1–2] In the case of highly fluorinated polymer materials, they do exhibit particular merits such as high thermal and weather resistance, excellent chemical inertness, oil and water repellency, and low dielectric index, in some cases, as well as biocompatibility.[3] Thus fluorinated (co)polymers have attached more interest in applications: the textile,[4] leather,[5] and paper industry as water and oil resistant coatings, as well as the surface protection[6] of stone, concrete, glass, and other inorganic substrates, especially for the protection of antiques.

But fluorinated polymers show two drawbacks that restricted their utilization severely: the high cost and weak adhesion property. Recently, those containing perfluoroalkyl side chains have been the focus of numbers of studies because of the good adhesion to matrices and the good reactivity of perfluoroalkyl acrylate with fluorine-free acrylate, which possibly reduces the cost.[7–11]

Demanding in terms of performance and environmental issues, the emulsion (co)polymerization of FA copolymers was favored. But compared with conventional surfactant, a reactive surfactant is not physically but chemically bond to the surfaces of latex to impart stronger stabilities.[12,13] Furthermore, the reactive surfactant can overcome some detrimental effects of conventional ones on the physical properties of the final polymer.

The aim of this work was to study the effects of concentrations of AMPSNa, KPS, FA as well as polymerization temperature on the kinetic features (rate of polymerization) and colloidal characteristics (mean particle diameter, particle disperse index, particle numbers, and surface charge density) of a soap-free emulsion copolymerization of FA. Furthermore, NMR, FTIR, AFM, and fluorine-selective electrode analysis were used to characterize the composition and morphology of the FA copolymers.

EXPERIMENTAL

Materials

Perfluoroalkyl acrylate ($CH_2{=}CH_2COOCH_2CH_2(CF_2)_7CF_3$) (97%) purchased from Aldrich was used directly. Methyl methacrylate (MMA) and *n*-butyl acrylate (*n*-BA) were washed with 5 wt % aqueous NaOH and deionized water, then distilled under vacuum prior to use. Potassium persulfate (KPS) was purified by recrystallization. Sodium 2-acrylamide-2-methyl propanesulfonate (AMPSNa), a kind gift from Lutozol, was used without further purification.

Correspondence to: S.-Y. Cheng (scheng@public.wh.hb.cn).

Journal of Applied Polymer Science, Vol. 104, 2438–2444 (2007)

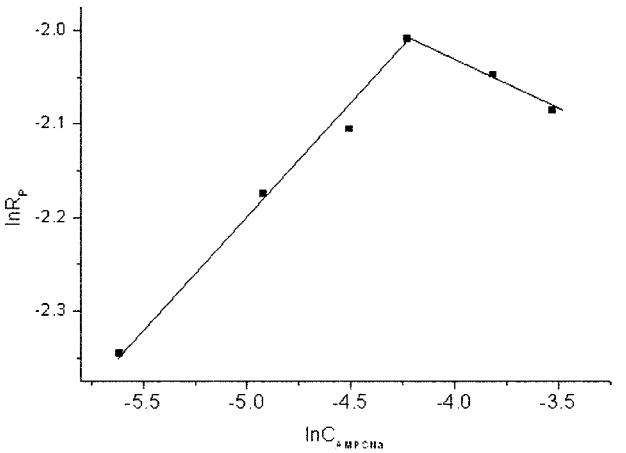

Figure 1 The relationship between ln Rp and ln C_{AMPSNa}. C_{AMPSNa}: 0.365, 0.73, 1.10, 1.46, 2.20, 2.93 $\times$ 10^{-2} mol/L; C_{KPS}: 7.33 m*M*; C_{FA}: 2.84 m*M*; *T*: 347 K.

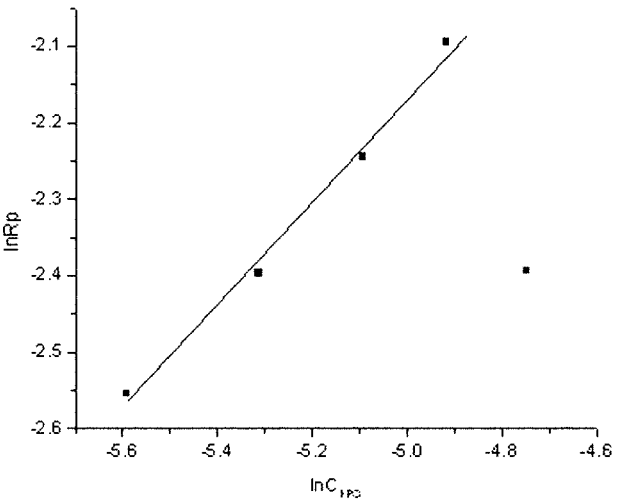

Figure 2 The relationship between ln Rp and ln C_{KPS}. C_{KPS}: 3.73, 4.93, 6.13, 7.33, 8.67 m*M*; C_{AMPSNa}: 1.46 $\times$ 10^{-2} mol/L; C_{FA}: 2.27 m*M*; *T*: 347 K.

Deionized water was used in all the preparation and characterization process.

Polymerization process

The polymerizations were performed in 0.25-L four-necked kettle equipped with mechanical stirrer, thermometer, reflux condenser, and inlet system of nitrogen. The stirring speed was about 300 rpm, and the polymeric temperature was in the range of 70–80°C. 65 mL deionized water, 10 g MMA, 15 g *n*-BA, as well as variable amount of AMPSNa and FA were charged into the kettle, followed by carefully removing oxygen by purged 30 min nitrogen. Then, the resulted pre-emulsion was added 10 mL initiator aqueous solution and then heated to $\sim$ 74°C for 4 h yielding stable latex. The rates of polymerization (R_p) were calculated from the instantaneous conversions of monomers. The instantaneous conversion was defined as a ratio of the polymer formed to the monomer fed at that time and determined gravimetrically.

Latex characterization

The diameters (D_w) of synthesized latex particles were obtained by Photo Correlation Spectroscopy (Auto Size Loc-Fc963, Malven). PDI referred to the particle disperse index, and smaller the PDI values, the narrower the distribution of particle size was. The particle numbers per microliter water (N_p) was calculated with obtained D_w. The surface charge density was determined by conductimetric titration, with consideration given to the concentration of the titration agent (NaOH) and the surface area of the latex particles. The morphology of lattices was characterized by transmission electron microscopy (TEM), which was taken with a TEX-100SX instrument operating at 10 kV.

Structural characterization

The fluorine content in the copolymer was determined by fluorine-selective electrode analysis and NaF solutions in different concentrations (from 10^{-2} to 10^{-5} mol/L) were used to create a standard curve. FTIR spectrum of ultra-thin copolymer films was recorded on PerkinElmer FTIR spectrometer. ^{1}H, ^{19}F-NMR were measured on an INOVA 600 MHz spectrometer at 25°C in chloroform-*d*. The values of chemical shifts for ^{19}F-NMR are stated downfield from trifluorotrichloroethane.

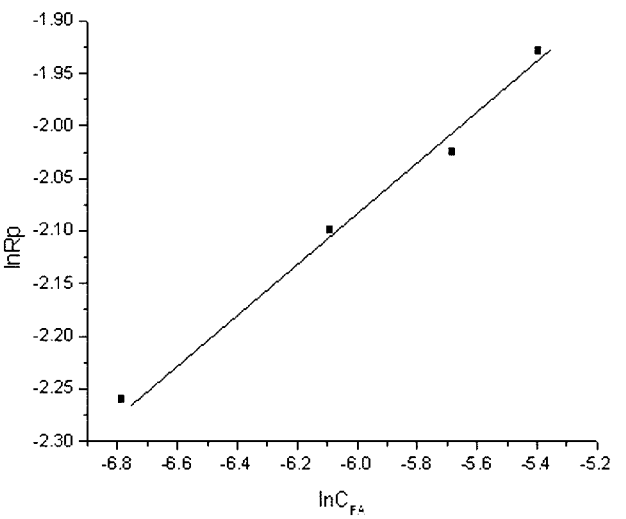

Figure 3 The relationship between ln Rp and ln C_{FA}. C_{FA}: 1.13, 2.27, 3.40, 4.53 m*M*; C_{AMPSNa}: 1.46 $\times$ 10^{-2} mol/L; C_{KPS}: 7.33 m*M*; *T*: 347 K.

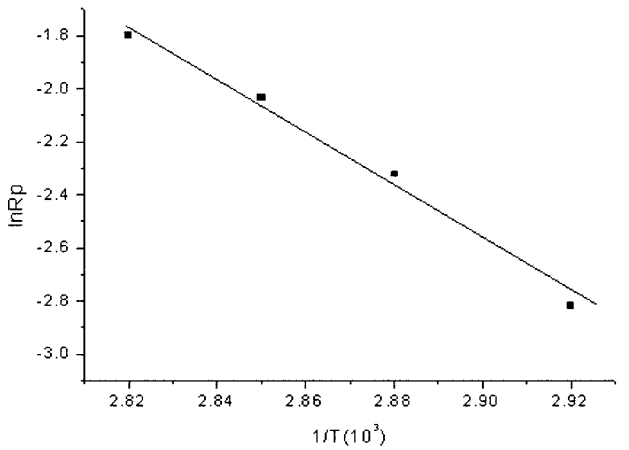

Figure 4 The relationship between ln Rp and $1/T$. T: 343, 347, 351, 355 K; C_{AMPSNa}: 1.46×10^{-2} mol/L; C_{KPS}: 7.33 mM; C_{FA}: 2.27 mM.

Surface characterization

Water resistance was characterized by soaking polymer films in water at room temperature and weighing the amount of water absorbed at a present time (72 h) period. Sample size was 2.0 cm in length, 1.5 cm in width, and 0.60 ± 0.10 mm in thickness. Water absorption was defined as $W_a\% = (W - W_0)/W_0$, where W_0 is the weight before soaking and W is the weight after soaking. The smaller the values of $W_a\%$, the better the water resistance of films are. The reported values were the average of three measurements made at different positions of a film.

Aqueous contact angles (θ) dates of latex films were taken by Wilhelmy method[14] at 25°C by a Krüss interface tension meter (Krüss, Hamberg, Germany). The sample was progressively immersed into the hexane or water at a constant rate, the former aimed to provide the wetting length of samples. The plates were immersed at the speed of 0.5 mm/s into the water.

Thin films were prepared by spin coating in a freshly cleaved mica plate. AFM measurements were obtained with a Nanoscope IIIa (Digital Instrument, Santa Barbara, CA). All measurements were made in the tapping mode.

RESULTS AND DISCUSSION

Kinetics features of FA soap-free emulsion copolymerization

To obtain the optimal reaction condition for the soap-free copolymerization of perfluoroacrylate using AMPSNa as a reactive surfactant, several parameters, namely concentrations of AMPSNa, KPS, and FA, as well as polymerization temperature, were studied.

The ln R_p versus ln C_{AMPSNa} plot with six different AMPSNa concentrations was reported in Figure 1, showing a sharp increase in the rates of polymerization when C_{AMPSNa} increasing from $0.365 \times 10^{-2}M$ to $1.46 \times 10^{-2}M$, but then a slight decrease when C_{AMPSNa} surpassing $1.46 \times 10^{-2}M$. With increasing AMPSNa concentration, the monomer concentration in aqueous phase increased and then the numbers of primary particles increased. It is known that R_p is linearly proportional to particle numbers, so R_p finally went up. The second reason was related to viscosity's increase resulted by the ionic association of polar groups for introduction of AMPSNa, which brought about the diffusion-controlled rate of termination went down, that was, the rate of polymerization went up. But when C_{AMPSNa} was excessive, the resulting oligomer radicals presented too many charges and too hydrophilic to absorb onto the surfaces of primary particles in time, which delayed capturing radicals and finally R_p decreased. So, there existed two exponential order of correspondence between R_p and C_{AMPSNa}: 0.23 and −0.11 below and above $1.46 \times 10^{-2}M$.

In Figure 2, the effect of concentrations of initiator on rates of polymerization was shown. Except for the concentration of initiator of 8.67 mM, R_p increased with C_{KPS}. In the case of 8.67 mM, a significant amount of copolymer coagulum formed during the self-accelerating period, because the inlet temperature in the reactor increased sharply resulted from the decomposition heat of superfluous initiator, to damage system stability. $R_p \propto C_{KPS}^{0.68}$ was obtained by using linearity regression of the anterior four points in Figure 2. The obtained 0.68 order was higher than

TABLE I
Effects of C_{AMPSNa} on Colloidal Characteristics of Latexes

C_{AMPSNa} (10^2 mol L^{-1})	D_w (nm)	PDI	N_p (10^{-15} mL^{-1} H_2O)	Surface charge density (μmol m^{-2})
0.365	156.4	0.018	0.135	0.55
0.73	134.8	0.017	0.209	0.55
1.10	130.1	0.024	0.232	0.58
1.46	125.1	0.028	0.271	0.59
2.20	144.0	0.032	0.172	0.68
2.93	152.3	0.039	0.145	0.87

C_{KPS}: 7.33 mmol/L; C_{FA}: 2.84 mmol/L; T: 347 K.

TABLE II
Effects of C_{KPS} on Colloidal Characteristics of Latexes

C_{KPS} (mmol L^{-1})	D_w (nm)	PDI	N_p (10^{-15} $mL^{-1}H_2O$)	Surface charge density (μmol m^{-2})
3.73	138.5	0.020	0.185	0.39
4.93	134.0	0.035	0.200	0.46
6.13	130.1	0.107	0.220	0.47
7.33	139.2	0.010	0.180	0.59
8.67	153.6	0.025	0.153	0.56

C_{AMPSNa}: 1.46×10^{-2} mol/L; C_{FA}: 2.27 mmol/L; T: 347 K.

the value of 0.5 given by the classical Smith-Ewart theory, which maybe attributed to the indirectly prolonged half-life of free radicals because the increase of viscosity in single latex had delay a diffusion-controlled rate of termination.

The effect of various FA concentrations on copolymerization kinetics was also examined in Figure 3 and the dependency between R_p and C_{FA} was 0.23. Figure 4 shows that R_p increased with rising polymerization temperature, and the apparent activation energy was 84.99 kJ/mol calculated by the Arrhenius equation.

Latex characterization

In Tables I and II, it was clear that the particle size decreased first, and then increased upon increasing AMPSNa and KPS concentration, and the particle numbers N_p indicated the opposite trend. Furthermore, the lattices were rather monodisperse (Fig. 5), which confirmed again by the PDI data depicted. These results can be interpreted by the consideration of two factors: one is that the final number of primary particles increased, the other is that more aggregation of the newly nucleated particles occurred because of the reduction in the electrostatic repulsion.

Tables I and II also show the values of surface charge density of final latex particles. The experimental values were similar to the expected ones calculated according to the raw materials. However, the results showed that the higher the D_w was of the anionic lattices, the higher the surface charge was. This was due to the fact that for the same amount of polymer formed when the D_w was higher, the total surface area of the particles was higher and the more charge was distributed over a larger area.

With addition fluorinated monomer FA, limited aggregation of the newly nucleated particles occurred because of the reduction in the surface energy of polymer resulted by the introduction of perfluoroalkyl groups, thus D_w increased gradually with increasing FA concentration (Table III). Table IV shows that particle size of lattices increased and number of particles decreased with rising temperature. Maybe the opportunity of collision of the newly nucleated particles increased with rising temperature.

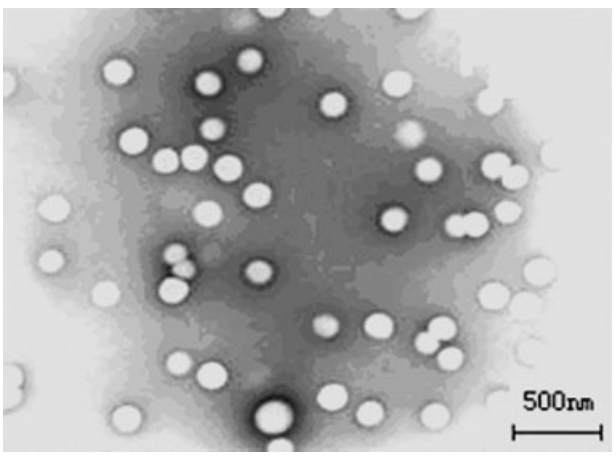

Figure 5 Transmission electron microscopy graphs of the lattices. The polymerization condition: C_{AMPSNa}: 1.46×10^{-2} mol/L; C_{KPS}: 7.33 mM; C_{FA}: 2.27 mM; T: 347 K.

Structural characterization

The polymer films were extracted in trichlorotrifluoroethane solvent for 24 h to remove most of the unreacted FA monomer/homopolymer possibly presenting in the films. The structure and composition of the worked FA copolymers were confirmed by combination of different techniques.

The calculated and measured fluorine content versus C_{FA} was plot in Figure 6, which obviously

TABLE III
Effects of C_{FA} on D_w and N_p

C_{FA} (mmol L^{-1})	D_w (nm)	PDI	N_p (10^{-15} mL^{-1} H_2O)
0	128.2	0.012	0.236
1.13	133.7	0.028	0.222
2.27	139.2	0.010	0.197
3.40	144.6	0.019	0.193
4.53	145.9	0.068	0.186

C_{AMPSNa}: 1.46×10^{-2} mol/L; C_{KPS}: 7.33 mmol/L; T: 347 K.

TABLE IV
Effects of Polymerization Temperature on D_w and N_p

T (K)	D_w (nm)	PDI	N_p (10^{-15} mL^{-1} H_2O)
343	130.7	0.073	0.232
347	139.2	0.010	0.197
351	142.0	0.039	0.183
355	145.5	0.079	0.172

C_{AMPSNa}: 1.46 × 10^{-2} mol/L; C_{KPS}: 7.33 mmol/L; C_{FA}: 2.27 mmol/L.

indicated the calculated ones were higher than the measured ones. The two possible reasons had been proposed: One was the loss of fluorine during the burning process absorbed by the glass-made oxygen bomb; the other was the existence of FA homopolymer trace.

In the IR spectrum of FA copolymer as shown in Figure 7, the first wide region of interest lies between 1100 and 1300 cm^{-1}, which is dominated by bands associated with motions of the CF_2 group at 1260 cm^{-1}. In addition, the band at 1220 cm^{-1} is attributed to stretching and bending of carbon skeleton of the fluorocarbon helix. In the second region of interest are there two medium bands at 660 and 710 cm^{-1}, which result from a combination of rocking and wagging vibration of CF_2 groups.

Figure 8(a) is a typical ^{1}H-NMR spectrum of the resulted FA copolymer. A —COOC**H**$_2$— peak at δ 4.034 ppm due to the FA in the polymer chain is observed, and another peak at δ 1.813 ppm is assigned to R_fC**H**$_2$—. The structure of FA is so similar to MMA and *n*-BA that the other proton peaks almost overlap each other. The ^{19}F-NMR spectrum of the copolymers depicted in Figure 8(b) confirmed the presence of three different kinds of fluorine resonances originating from the perfluoroalkyl side chains.

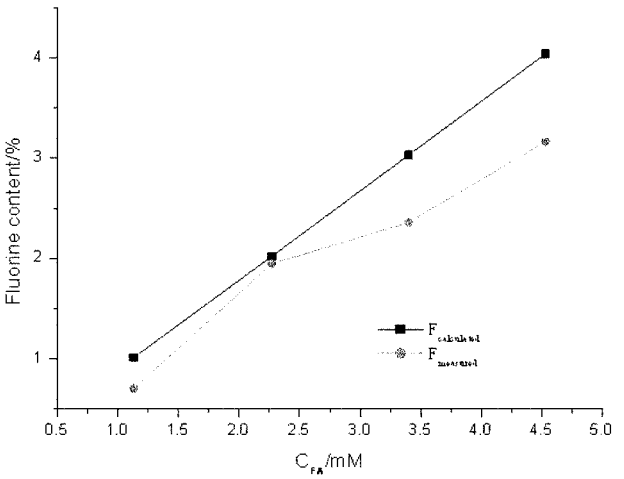

Figure 6 The plot of calculated and measured fluorine content versus C_{FA}.

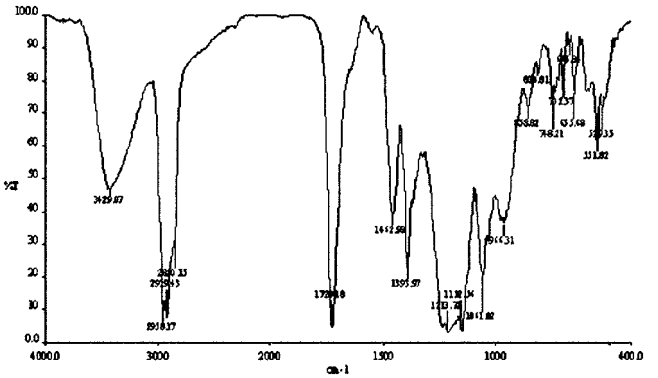

Figure 7 FTIR spectra of the FA copolymer latex films with FA concentration of 2.27 m*M*.

The chemical shifts are −81.5 ppm (t, 3F) of end-C**F**$_3$ group, −114.5 ppm (t, 2F) of —CH_2C**F**$_2$— group, and −121 to −125 ppm of —$(CF_2)_5$, respectively.

Surface characterization

The effect of varying FA concentrations on surface property of the resulted copolymers was studied using aqueous contact angles, water resistance, and atomic force microscopy (AFM).

As shown in Table V, the water resistance of the FA copolymer films improved dramatically, by say,

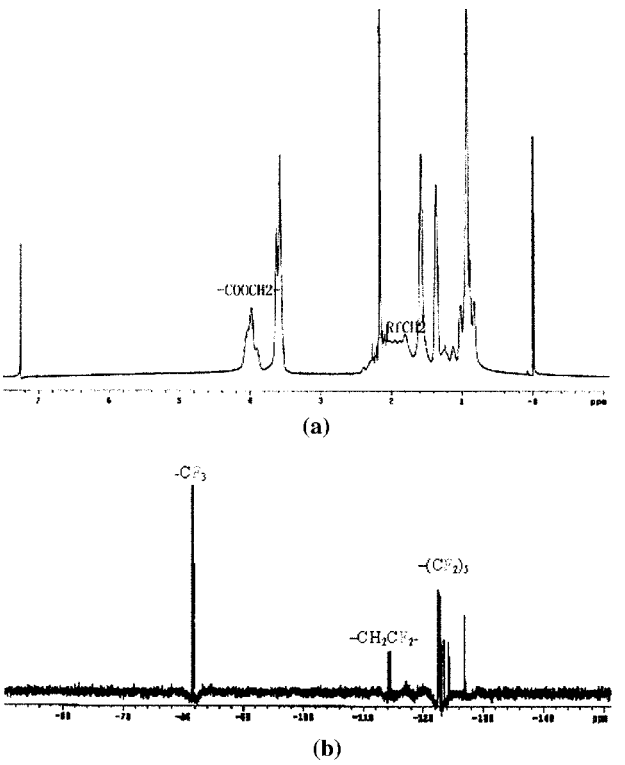

Figure 8 (a) ^{1}H-NMR spectrum of FA copolymer latex film with FA concentration of 2.27 m*M*. (b) The ^{19}F-NMR spectra of FA copolymer with FA concentration of 2.27 m*M*.

TABLE V
Effects of the FA Concentration on Contact Angle and Absorption Ratio for Water

C_{FA} (mmol L^{-1})	θ	W_a (%)
0	69.5 ± 2.0	28.12 (SD 0.80)
1.13	92.8 ± 2.0	16.94 (SD 2.14)
2.27	98.0 ± 1.5	13.20 (SD 1.78)
3.4	102.0 ± 2.0	9.58 (SD 0.97)
4.53	107.1 ± 1.0	11.41 (SD 0.98)
3.40[a]	103.3	15.7

[a] Synthesis by conventional emulsion polymerization.

the absorption ratio of water decreased, with FA addition. For instance, the absorption ratio of water for a FA-free polymer was 28.12 wt %, whereas the absorption ratio of water for the FA-containing one decreased by about 15 wt % indicating the water resistance further improved. Compared with the copolymers prepared by conventional emulsion polymerization, the water resistance of latex films was greatly improved too.[7]

A common empirical method for measuring wettability is to obtain a contact angle, because theoretically, it is sensitive to the outermost surface atoms or molecules. Table V also shows that the aqueous contact angles for FA copolymer films had been found much increase when compared with those of fluorine-free copolymers. For example, the θ for fluorine-containing films was above 90°. However, the corresponding θ for fluorine-free one was only 69.5°. The self-assembly of the perfluoroalkyl chains occurred at the water–air interface in the film-forming process. The aqueous contact angles are the most sensitive to the nonwettable portions of the surface. There was an increase in aqueous CA values with increasing FA weight concentrations.

Usually an increase in aqueous contact angles indicated an increased hydrophobicity. The fluorinated polymer has low surface energy property, and incorporation of fluorinated moieties into a polymer film has been shown to be effective for increasing the hydrophobicity of film's surface. The surface free energy of the polymers was calculated using measured contact angles for various liquids by eqs. (1) and (2):

$$\gamma_{\text{solid}} = \gamma^d_{\text{solid}} + \gamma^p_{\text{solid}} \tag{1}$$

$$\gamma_{\text{liquid}}(\cos\theta + 1) = 2\left(\gamma^d_{\text{solid}}\gamma^d_{\text{liquid}}\right)^{1/2} + 2\left(\gamma^p_{\text{solid}}\gamma^p_{\text{liquid}}\right)^{1/2} \tag{2}$$

where γ is the surface free energy, and the superscripts d and p correspond to dispersion and polar components of the surface free energy, respectively. The surface free energy of the FA copolymer films was evaluated about 14.38 mN/m using water and diiodomethane as wetting solvent when fixing FA concentration to 4.53 mM.

To investigate the distribution of surface composition, atomic force microscopy (AFM) was used to evaluate the topography of the resulted films. The root-mean-square roughness values for AFM images (2 μm × 2 μm area) for various FA concentrations were about 0.75 nm. There are no striking morphology differences between the polymer surface AFM images. According to the AFM analysis in Figure 9, the upper layer of the FA copolymer film exhibited nanodomain-like superstructures, and the surface appeared ''bumpy'' with a grainy structure. This is again the result of phase separation of the lipophilic carbon–hydrogen groups and the perfluoroalkyl ones. Basically, the interaction between acrylate polymers and the polar mica substrate is stronger than the interaction between perfluorinated long groups and mica surface and will collapse on a mica surface. Solvent evaporation may induce the perfluoroalkyl side chains preferred to migrate to the air/polymer interface and occupy the outmost surface, and aggregate individual chains into the observed ''islands.''

CONCLUSIONS

The kinetics features of soap-free emulsion copolymerization of perfluoroalkyl acrylate, methyl methacrylate, and *n*-butyl acrylate, were analyzed. The rates of polymerization (R_p) were affected largely by AMPSNa, KPS, and FA concentration as well as

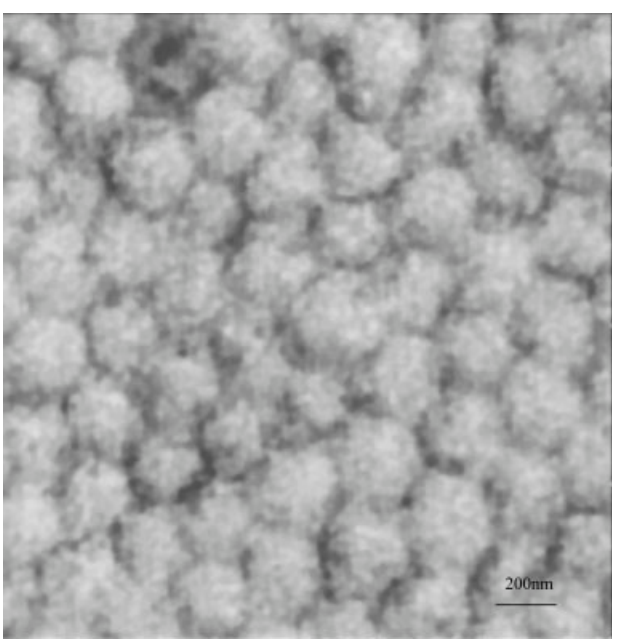

Figure 9 AFM images of latex films with fluorinated monomer addition of 2.27 mM (scan range: 2 × 2 μm^2).

polymerization temperature. The latex particles size growth was strongly attributed to the limited aggregation of the newly nucleated particles occurred. The enrichment of long perfluoroalkyl side chains on the surface of copolymers films, confirmed by AFM graphs, created copolymer films with lower surface energy as revealed by a high aqueous contact angle on the order of 100° and improved water resistance.

References

1. Yamabe, M. Makromol Chem Macromol Symp 1992, 64, 11.
2. Boutevin, B.; Ameduri, B. Makromol Chem Macromol Symp 1994, 82, 1.
3. Lynn, M. M.; Worm, A. T. In Encyclopedia of Polymer Science and Engineering, 2nd ed.; Mark, H. F.; Bikales, N. M.; Overberger, C. G.; Menzes, G., Eds.; Wiley: New York; 1987, Vol. 7, p 256.
4. Boutevin, B.; Diaf, K. O.; Pietrasanta, Y.; Taha, M. J Polym Sci, Part A: Polym Chem 1986, 24, 3129.
5. Bonardi, C. (to Atochem) Eur. Pat. Appl. 426530 (1991). Chem Abstr 1991, 115, 161338z.
6. Alessandrini, G.; Aglietto, M.; Castelvetro, V.; Ciardelli, F.; Peruzzi, R.; Toniolo, L. J Appl Polym Sci 2000, 76, 962.
7. Peng, H.; Yang, T. T.; Liao, Q. J.; Cheng, S. Y.; Park, I. J. Chinese J Appl Chem 2005, 22, 188.
8. Cheng, S. Y.; Chen, Y. J.; Chen, Z. G. J Appl Polym Sci 2002, 85, 1147.
9. Cheng, S. Y.; Chen, Y. J.; Wang, K. L. Acta Polymerica Sinic 2002, 5, 560.
10. Park, I. J.; Lee, S. B.; Choi, C. K. J Appl Polym Sci 1994, 54, 1449.
11. Chen, Y. J.; Zhang, C. C.; Cheng, S. Y. J Appl Polym Sci 2003, 90, 3609.
12. Xu, Z. S.; Yi, C. F.; Lu, G. H.; et al. Polym Int 1997, 44, 149.
13. Tang, G. L.; Song, M. D.; Hao, G. J.; et al. J Appl Polym Sci 2001, 79, 21.
14. Hogt, A. H.; Gregonia, D. F.; Andrade, J. D. J Colloid Interface Sci 1985, 106, 289.